



HHS Public Access

Author manuscript

Nat Neurosci. Author manuscript; available in PMC 2014 December 01.

Published in final edited form as:

Nat Neurosci. 2014 June ; 17(6): 804–806. doi:10.1038/nn.3710.

Cellular Origins of Auditory Event-Related Potential Deficits in Rett Syndrome

Darren Goffin¹, Edward S. Brodtkin², Julie A. Blendy³, Steve J. Siegel², and Zhaolan Zhou^{1,*}

¹Department of Genetics, Perelman School of Medicine, University of Pennsylvania, Philadelphia, PA 19104

²Department of Psychiatry, Perelman School of Medicine, University of Pennsylvania, Philadelphia, PA 19104

³Department of Pharmacology, Perelman School of Medicine, University of Pennsylvania, Philadelphia, PA 19104

Abstract

Dysfunction in sensory information processing is a hallmark of many neurological disorders including autism spectrum disorders (ASDs), schizophrenia and Rett syndrome (RTT)¹. Using mouse models of RTT, a monogenic disorder caused by mutations in *MECP2*², we demonstrate that the large scale loss of MeCP2 from forebrain GABAergic interneurons leads to deficits in auditory event-related potentials (ERPs) and seizure manifestation; but the restoration of MeCP2 in specific classes of interneurons ameliorates these deficits.

Sensory information processing, or the ability to accurately interpret and convert environmental stimuli into appropriate thoughts and decisions, represents a core domain of social behavior and cognitive function¹. Despite diverse genetic etiologies, deficits in sensory information processing, measured as changes in auditory or visual ERPs, represent an endophenotype commonly shared among patients with RTT, ASDs and schizophrenia^{1,3}. Similar deficits in ERPs are also observed in mouse models of RTT concomitant with the manifestation of behavioral abnormalities^{4,5}. However, the cellular origins and neural mechanisms underlying ERP deficits are poorly understood.

We therefore sought to dissect the causally important alterations in neural circuits and cellular origins of auditory ERP deficits in mouse models of RTT. We bred floxed MeCP2 mice (*Mecp2*^{2lox/+})⁶ with mice expressing Cre-recombinase under the control of the *Dlx5/6* enhancer to remove MeCP2 from forebrain GABAergic neurons⁷, or the *Emx1* promoter to remove MeCP2 from forebrain glutamatergic neurons and glia⁸ (Fig. 1a). We then examined ERPs by recording hippocampal local field potential (LFP) responses to auditory events consisting of white noise pips in awake, freely mobile mice. Wild-type (*Mecp2*^{2lox/y}, WT)

Users may view, print, copy, and download text and data-mine the content in such documents, for the purposes of academic research, subject always to the full Conditions of use:http://www.nature.com/authors/editorial_policies/license.html#terms

*Correspondence and requests for materials should be addressed to: Z.Z. (zhaolan@mail.med.upenn.edu).

The authors declare no competing financial interest.

mice exhibited a stereotypical decrease in event-related power at low frequencies and increase in event-related power at high frequencies, similar to previous findings⁴ (Fig. 1b and c). We also observed a robust increase in phase-locking factor (PLF), a measure of trial-to-trial reliability, across all frequencies (fig. S1). In contrast, *Mecp2*^{2lox/y}; *Dlx5/6-Cre* mice exhibited a marked and significant reduction in event-related power and PLF responses across all frequencies relative to WT mice (Fig. 1b, c and S1; permutation test with FDR < 0.05). These alterations were not the result of altered hearing since auditory brainstem responses, an evoked measure of activity in the brainstem used to assess hearing in humans and mice⁹, were unaffected (fig. S2).

In comparison, *Mecp2*^{2lox/y}; *Emx1-Cre* mice, which lack MeCP2 in forebrain glutamatergic neurons and glia, exhibited auditory-evoked power and PLF responses that were indistinguishable from those observed in WT littermates (Figs. 1a, b and S1). Basal oscillations in the high frequency range, however, were elevated in mice lacking MeCP2 from either glutamatergic or GABAergic neurons, similar to that observed in *Mecp2*-null mice⁴ (fig. S3). Since *Dlx5/6-Cre* exhibits recombination in forebrain GABAergic interneurons and striatal medium spiny neurons (MSNs)^{7,10}, we next conditionally deleted MeCP2 from either D1- or D2-dopamine receptor-expressing MSNs¹¹. We found that auditory-evoked power and PLF were unaffected by loss of MeCP2 from either population of MSNs (fig. S4). These data therefore suggest that loss of MeCP2 from forebrain GABAergic interneurons is primarily responsible for the observed deficits in auditory ERPs in mouse models of RTT.

Previous work found that loss of MeCP2 from forebrain GABAergic neurons results in motor incoordination, ataxia and altered social interactions¹². In contrast, we found that *Mecp2*^{2lox/y}; *Emx1-Cre* mice exhibited a significant decrease in locomotor activity ($p = 0.043$, two-tailed t-test with Welch's correction), but no significant alterations in motor coordination on an accelerating rotarod, anxiety-like behavior, social interactions or episodic learning and memory (fig. S5). Thus, MeCP2 in the forebrain appears to be critical for motor control, but auditory ERPs and social behaviors are particularly sensitive to MeCP2 function in forebrain GABAergic neurons.

Seizures represent one of the most debilitating symptoms in RTT¹³. However, mouse models of RTT show few, if any, behavioral seizures. We found that *Mecp2*^{2lox/y}; *Dlx5/6-Cre* mice frequently exhibited behavioral seizures that were recurring and lasted 10–60 seconds following routine handling of the mice after 3 months of age (Fig. 1d and videos S1–3). EEG recordings revealed electrographic seizures consisting of 6–8 Hz spikes and wave discharges (SWD) that were associated with behavioral arrest in *Mecp2*^{2lox/y}; *Dlx5/6-Cre* mice (Fig. 1e). In contrast, we have not detected behavioral or electrographic seizures in WT or *Mecp2*^{2lox/y}; *Emx1-Cre* mice despite prolonged monitoring at these ages. Together, these data suggest that loss of MeCP2 from forebrain GABAergic neurons leads to hyperexcitability that manifests as seizures.

We next examined whether the preservation of MeCP2 function in forebrain GABAergic neurons is sufficient to maintain normal auditory ERPs in otherwise *Mecp2*-null mice. We therefore bred *Dlx5/6-Cre* and *Emx1-Cre* mice with mice containing a floxed transcriptional

Stop sequence in the endogenous *Mecp2* gene (*Mecp2^{Stop}*)¹⁴. We confirmed that MeCP2 is expressed in the majority of GAD67-expressing neurons in *Mecp2^{Stop/y}; Dlx5/6-Cre*, but not *Mecp2^{Stop/y}; Emx1-Cre* mice (fig. S6). Similar to our previous studies in *Mecp2*-null mice⁴, we found that auditory-evoked neural responses were markedly and significantly reduced in *Mecp2^{Stop/y}* mice compared to their WT littermates (Fig. 2 and fig. S7; permutation test; FDR < 0.05). Remarkably, recordings in *Mecp2^{Stop/y}; Dlx5/6-Cre*, but not *Mecp2^{Stop/y}; Emx1-Cre* mice, revealed a significant preservation of auditory-evoked power and PLF compared to *Mecp2^{Stop/y}* mice (Fig. 2 and fig. S7; permutation test; FDR < 0.05). Furthermore, *Mecp2^{Stop/y}; Emx1-Cre* mice, where MeCP2 expression is preserved in most forebrain neurons and glia except GABAergic neurons, showed behavioral seizures around 2 months of age (video S4). Notably, the marked RTT-like phenotypes and decreased longevity in *Mecp2^{Stop/y}* mice are not rescued by selective preservation of MeCP2 in forebrain glutamatergic or GABAergic neurons (fig. S8), which is likely due to the absence of MeCP2 from mid- and hindbrain regions that control respiration and autonomic function^{12,15}. Together, these results further demonstrate that MeCP2 function in forebrain GABAergic neurons is required for maintaining proper auditory ERPs and preventing seizure manifestation.

To further evaluate the GABAergic interneuron cell types mediating these effects, we examined the contributions of MeCP2 in Parvalbumin (PV)- and Somatostatin (SOM)-expressing interneurons by conditionally deleting MeCP2 from PV- or SOM-expressing interneurons using *PV-Cre*¹⁶ or *SOM-Cre*¹⁷ mouse lines. We found that auditory-evoked power and PLF (fig. S9) in *Mecp2^{2lox/y}; PV-Cre* or *Mecp2^{2lox/y}; SOM-Cre* mice were indistinguishable from that of their WT littermates. In addition, we did not observe any behavioral seizures, overt RTT-like abnormalities or decreased longevity in these mice. Strikingly, however, we found that the selective preservation of MeCP2 in either PV- or SOM-expressing interneurons led to a significant preservation of auditory-evoked power and PLF compared to *Mecp2^{Stop/y}* mice (Fig. 3a, b and fig. S10; permutation test with FDR < 0.05). Previous work suggests that soma-targeting PV interneurons regulate the output firing of pyramidal neurons, whereas the dendrite-targeting SOM-expressing interneurons modulate the input to these neurons^{18–20}. Restoring MeCP2 function in either PV- or SOM-expressing interneurons may therefore be sufficient to partially restore proper pyramidal neuron activity and thus help stabilize auditory ERPs. Preservation of MeCP2 in either PV- or SOM-expressing interneurons also ameliorated overt RTT-like behavioral phenotypes (Fig. 3c; $p < 0.001$, one-way ANOVA with post-hoc Tukey test) and prolonged longevity in *Mecp2^{Stop/y}* mice (Fig. 3d). This is likely due to the restored expression of MeCP2 in PV or SOM interneurons that are widely distributed throughout the brain.

In summary, our findings demonstrate that MeCP2 function in forebrain GABAergic, but not glutamatergic, neurons is required for generating auditory ERPs. Additionally, loss of MeCP2 function in GABAergic neurons by either ablation of MeCP2 from GABAergic neurons, or preservation of MeCP2 in glutamatergic neurons in *Mecp2*-null mice, leads to cortical hyperexcitability and behavioral seizures. Furthermore, we found that deficits in auditory ERPs occur following the large-scale loss of MeCP2 from forebrain GABAergic interneurons; but restoration of MeCP2 function in either PV- or SOM-expressing

interneurons can ameliorate these deficits. Our findings thus provide a platform for exploring these differential cellular influences on ERPs and for developing novel therapeutic strategies to alleviate sensory information processing impairments in ASDs, schizophrenia and RTT.

MATERIALS AND METHODS

Animals

Experiments were conducted in accordance with the ethical guidelines of the National Institutes of Health and with the approval of the Institutional Animal Care and Use Committee of the University of Pennsylvania. Floxed *Mecp2^{2lox/+6}*, *Mecp2^{Stop/+14}*, *Dlx5/6-Cre⁷*, *Emx1-Cre⁸*, *D1-Cre¹¹*, *D2-Cre¹¹*, *PV-Cre¹⁶*, *SOM-Cre¹⁷* were all obtained from Jackson laboratories. All animals were housed in a standard 12-hour light: 12 hour dark cycle with access to ample amounts of food and water. All experiments described were performed using animals on a congenic C57BL/6 background.

Surgical procedures

Each mouse was deeply anesthetized (1–2% isoflurane) and was mounted in a stereotaxic frame with non-puncturing ear bars. Three stainless steel electrodes, mounted in a single headstage, were aligned to the sagittal axis of the skull. A stainless steel recording electrode was placed 2.0 mm posterior, 2.0 mm left lateral relative to bregma and 1.8 mm depth. Ground and reference electrodes were placed anterior of the hippocampal electrode at 1.0 mm and 2.0 mm distances, respectively. The headstage was then fixed to the skull with screws with dental acrylic.

Data acquisition and analysis

ERP recordings were performed on freely mobile, non-anesthetized mice in their home cage environment after 20-minute acclimation to the recording room at 10–14 weeks of age. For local field potential recording, neural signals were acquired using Spike2 software connected to a Power 1401 II interface module (CED) and high impedance differential AC amplifier (A-M Systems). Signals were amplified (gain: 1,000), filtered (1–500 Hz) and sampled at 1.67 kHz. Auditory stimuli consisting of a series of 250 white-noise pips (10 ms duration, 85-dB SPL, 0.25 Hz frequency). Stimuli were presented through speakers on the recording chamber ceiling (Model 19-318A, 700–10,000 Hz frequency response, Radioshack) connected to a digital audio amplifier (RCA Model STAV3870, Radioshack). Stimuli were calibrated using a sound pressure meter. Due to frequency response of speakers, white noise has a corresponding bandwidth of 700 – 10,000 kHz. Analysis of event-related power and phase-locking factor (PLF) were performed similar to that described previously⁴, except instantaneous power and phase were calculated using wavelet methods with custom C routines. Event-related phase locking was measured using a PLF by calculating 1 – circular variance of instantaneous phase measurements, defined as:

$$PLF = 1 - \frac{1}{n} \sqrt{\sum_{k=1}^n (\cos\theta_k)^2 + \sum_{k=1}^n (\sin\theta_k)^2}$$

Auditory brainstem responses (ABR) recordings were performed using the same equipment and electrode placement as other recordings except EEG signals were acquired at 15.6 kHz. Auditory stimulation consisted of 4000 white-noise pips (3 ms duration, 8 Hz frequency) at 85-, 80-, 75-, 70-, 65-, 60- and 55-dB SPL. LFP signal was digitally filtered between 100 and 500 Hz and EEG amplitudes averaged across trials centered at t=0 seconds representing sound presentation.

For statistical analysis, event-related power and PLF were separated into frequency ranges with the mean power or PLF calculated between frequencies: δ , 2–4 Hz; θ , 4–8 Hz; α , 8–12 Hz; β , 12–30 Hz; γ_{low} , 30–50 Hz; γ_{high} , 50–90 Hz; ϵ , 90–140 Hz. Statistical significance was assessed using permutation tests based on t-statistics and false discovery correction made using the q-value methodology as previously described²¹.

Animal Behavior

All animal behavioral studies were carried out blinded to genotype. Mice were allowed to habituate to the testing room for at least 30 minutes prior to the test and testing was performed at the same time of day. All animal behaviors were performed on adult male littermates at 12–15 weeks of age.

Phenotypic scoring

Mice were scored for the absence or presence of RTT-like symptoms as described previously¹⁴. This test provides a semi-quantitative assessment of symptom status. Each of 6 symptoms was scored as 0 (absent or as wild-type), 1 (symptom present) or 2 (symptom severe). Symptoms assessed were mobility, gait, hindlimb clasping, tremor, breathing and overall condition. Symptoms were scored as previously described¹⁴. Mice were also weighed at each scoring session. Statistics were calculated using two-way ANOVA (genotype x phenotypic score) with Bonferroni's post hoc analysis.

Elevated zero maze

The elevated zero maze (Stoelting) consists of a circular-shaped platform elevated above the floor. Two opposite quadrants of the maze are enclosed (wall height, 12 inches), whereas the other two are open (wall height, 0.5 inches). Mice were placed in one of the closed quadrants and their movement traced over the course of 5 min. Analysis was performed with automated tracking software (TopScan software, Clever Systems). Statistics were performed using unpaired two-tailed t-test with Welch's correction to assume unequal variances.

Open field

Activity in an open field was quantified in a Plexiglas open-field box (43×43 cm²) with two sets of 16 pulse-modulated infrared photobeams (MED Associates, Georgia, Vermont). Data were analyzed based on total distance travelled and time spent in two zones: center (25% total area) and surround (75% total area). Statistics were performed using unpaired two-tailed t-test with Welch's correction to assume unequal variances.

Accelerating rotarod

Mice were placed on an accelerating rotarod apparatus (Med Associates) for 16 trials (4 trials a day on 4 consecutive days) with at least 15 min of rest between the trials. Each trial lasted for a maximum of 5 minutes, during which the rod was linearly accelerated from 3.5 to 35 rpm. The amount of time for each mouse to fall from the rod was recorded for each trial. Statistics were calculated using two-way ANOVA (genotype x trial).

Three-chamber social test

The three-chamber social test was conducted as described²². The test mice were introduced into the center chamber of the three-chambered apparatus and allowed to acclimate for 10 minutes. In the social choice test, a novel juvenile male (3–4 weeks of age, A/J mouse, The Jackson Laboratory) was introduced to the “social” chamber, inside a transparent Plexiglas cylinder containing multiple holes to allow for air exchange. In the other (non-social) chamber, a paperweight was placed in an identical empty cylinder. During the novel social test, a novel age-matched conspecific male mouse was introduced to the “novel” chamber, inside a cylinder as before. In the other (familiar) chamber, a cage mate control (whom the test mouse had been housed with since weaning) was placed in an identical cylinder. The designations of the social and non-social chambers or novel and familiar chambers were randomly chosen in each test to prevent chamber bias. Between tests, the chambers were cleaned with water and allowed to dry completely before initiating the next test. The time spent interacting (sniffing, climbing) the cylinders was quantified using automated tracking software (TopScan software, Clever Systems). Statistics were calculated using two-way ANOVA (genotype x trial).

Fear-conditioning

The fear-conditioning apparatus consisted of a conditioning cage (16×6×8 inches) with a grid floor wired to a shock generator and a scrambler, surrounded by an acoustic chamber. To induce fear-conditioning, mice were placed in the cage for 120 seconds, and then a pure tone (2 kHz) was played for 20 seconds, followed by a 2 second foot-shock (0.75 mA). Immediate freezing behavior was monitored for a period of 60 seconds, followed by a second tone and shock and freezing measurement taken once again for 60 seconds. Mice were then returned to their home cage. Fear-conditioning was assessed 24 hours later by a continuous measurement of freezing (complete immobility). To test contextual fear conditioning, mice were placed in the original conditioning cage and freezing was measured for 5 minutes. To test auditory-cued fear-conditioning mice were placed in a different context: the walls of the conditioning cage were altered, the floor grid covered and cage scented with almond. As a control for the influence of the novel environment, freezing was measured for 2 minutes in this new environment, and then a 2 kHz tone was played for 1 minute, during which conditioned freezing was measured. Statistics were calculated using two-way ANOVA (genotype x test).

Immunohistochemistry

Mice were deeply anesthetized (Avertin, 1.25%), perfused with 4% paraformaldehyde (PFA) in 0.1 M sodium-potassium phosphate buffered saline (PBS), and 20 μm coronal or

sagittal sections taken. Immunohistochemistry was performed on free-floating sections as previously described⁴ with the following antibodies: mouse anti-GAD67 (1:500; Millipore), mouse anti-PV (1:500; Millipore) and a custom rabbit anti-MeCP2 (1:1000)²³. All Immunohistochemistry experiments were successfully repeated in three different mice per genotype.

Statistics

Data are presented as mean \pm s.e.m. Statistical analyses were performed using GraphPad Prism software unless otherwise stated. Data distribution was assumed to be normal but this was not formally tested. Furthermore, variance was found to be similar between groups being statistically compared. No statistical methods were used to pre-determine sample sizes but our sample sizes are similar to those reported in previous publications^{4,22}. For all experiments, the experimenter was blind to genotype and samples were pseudo-randomized. No animals were excluded from analyses. A methods checklist is available with the supplementary materials.

Supplementary Material

Refer to Web version on PubMed Central for supplementary material.

Acknowledgments

The authors thank members of the Zhou lab for critical readings of the manuscript. This work was supported by NIH grants NS081054 and MH091850 (Z.Z.) and International Rett Syndrome Foundation (Z.Z. and D.G.). Z.Z. is a Pew Scholar in Biomedical Sciences. D.G. and Z.Z. designed the experiments and wrote the manuscript; D.G. conducted the experiments and performed data analysis. E.S.B. and J.A.B. helped design and interpret behavioral tests. S.J.S. helped design and interpret the electrophysiology studies.

References

1. Uhlhaas PJ, Singer W. *Neuron*. 2012; 75:963–980. [PubMed: 22998866]
2. Chahrour M, Zoghbi HY. *Neuron*. 2007; 56:422–437. [PubMed: 17988628]
3. Goffin D, Zhou Z. *Front Biol*. 2012; 7:428–435.
4. Goffin D, et al. *Nature neuroscience*. 2012; 15:274–283. [PubMed: 22119903]
5. Liao W, et al. *Neurobiol Dis*. 2012; 46:88–92. [PubMed: 22249109]
6. Chen RZ, Akbarian S, Tudor M, Jaenisch R. *Nat Genet*. 2001; 27:327–331. [PubMed: 11242118]
7. Monory K, et al. *Neuron*. 2006; 51:455–466. [PubMed: 16908411]
8. Gorski JA, et al. *J Neurosci*. 2002; 22:6309–6314. [PubMed: 12151506]
9. Hardisty-Hughes RE, Parker A, Brown SDM. *Nat Protoc*. 2010; 5:177–190. [PubMed: 20057387]
10. Zhao YT, Goffin D, Johnson B, Zhou Z. *Neurobiol Dis*. 2013; 59:257–266. [PubMed: 23948639]
11. Gong S, et al. *J Neurosci*. 2007; 27:9817–9823. [PubMed: 17855595]
12. Chao HT, et al. *Nature*. 2010; 468:263–269. [PubMed: 21068835]
13. Katz DM, et al. *Dis Model Mech*. 2012; 5:733–745. [PubMed: 23115203]
14. Guy J, Gan J, Selfridge J, Cobb S, Bird A. *Science*. 2007; 315:1143–1147. [PubMed: 17289941]
15. Ward CS, et al. *J Neurosci*. 2011; 31:10359–10370. [PubMed: 21753013]
16. Madisen L, et al. *Nature neuroscience*. 2010; 13:133–140. [PubMed: 20023653]
17. Taniguchi H, et al. *Neuron*. 2011; 71:995–1013. [PubMed: 21943598]
18. Isaacson JS, Scanziani M. *Neuron*. 2011; 72:231–243. [PubMed: 22017986]
19. Gentet LJ, et al. *Nature neuroscience*. 2012; 15:607–612. [PubMed: 22366760]

20. Lee SH, et al. *Nature*. 2012; 488:379–383. [PubMed: 22878719]
21. Storey JD, Tibshirani R. *Proc Natl Acad Sci USA*. 2003; 100:9440–9445. [PubMed: 12883005]
22. Wang ITJ, et al. *Proceedings of the National Academy of Sciences*. 2012; 109:21516–21521.
23. Zhou Z, et al. *Neuron*. 2006; 52:255–269. [PubMed: 17046689]

Author Manuscript

Author Manuscript

Author Manuscript

Author Manuscript

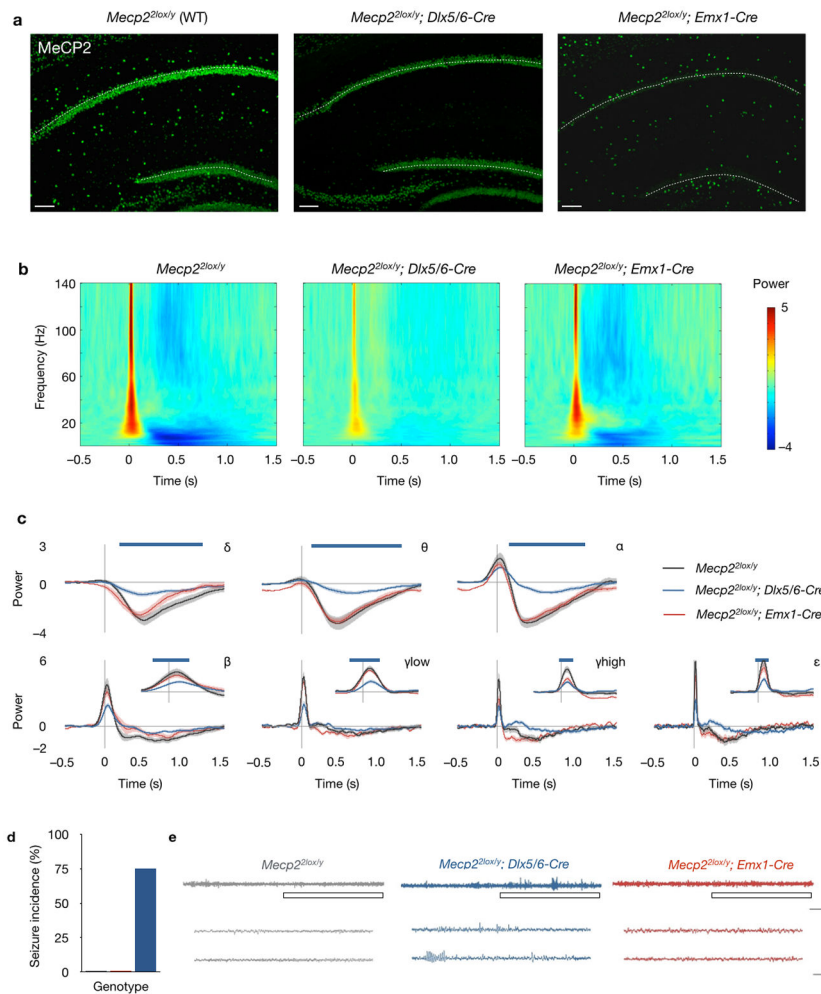


Fig. 1. MeCP2 function in forebrain GABAergic, but not glutamatergic neurons, is necessary for auditory information processing

(a) MeCP2 immunoreactivity in the hippocampus of wild-type (*Mecp2*^{2lox/y}) mice and those where MeCP2 has been conditionally deleted from forebrain GABAergic (*Mecp2*^{2lox/y}; *Dlx5/6-Cre*) or glutamatergic neurons (*Mecp2*^{2lox/y}; *Emx1-Cre*). Glutamatergic pyramidal and granule cell layers are marked by dotted white lines. Scale bars correspond to 100 μ m. These localization patterns were observed in three mice per genotype. (b) Heat maps showing changes in event-related power in response to 85-dB white noise sound presentation as a function of time and frequency. (c) Population averages of event-related power separated into frequency bands (δ , 2–4 Hz; θ , 4–8 Hz; α , 8–12 Hz; β , 12–30 Hz; γ_{low} , 30–50 Hz; γ_{high} , 50–90 Hz; ϵ , 90–140 Hz) for *Mecp2*^{2lox/y}; *Dlx5/6-Cre* mice (n = 13), *Mecp2*^{2lox/y}; *Emx1-Cre* mice (n = 7) and *Mecp2*^{2lox/y} mice (n = 9). Shaded regions represent s.e.m. Top blue bars represent those regions with FDR < 0.05 (permutation test). (d) The frequency of behavioral seizures. See supplementary information for videos of examples of these seizures. (e) Top, representative EEG traces from awake, freely mobile mice. Scale bar corresponds to 5 seconds (horizontal) and 200 μ V (vertical). Bottom traces are expanded views taken from boxed regions. Scale bar corresponds to 1 second (horizontal) and 200 μ V (vertical).

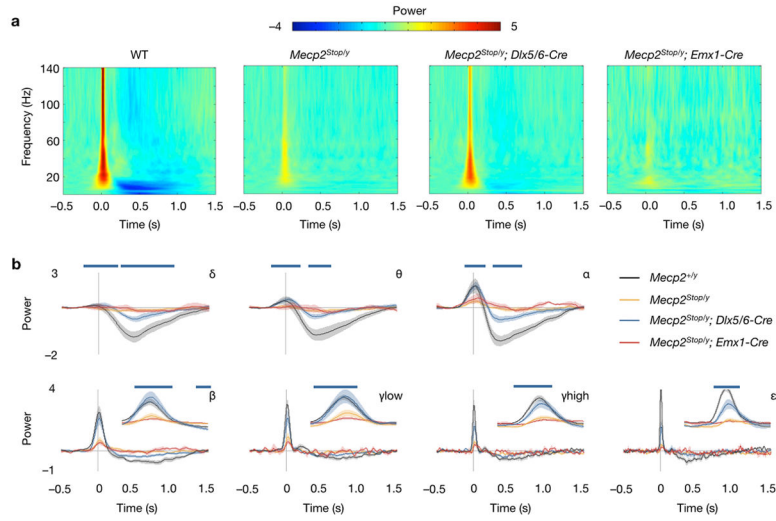


Fig. 2. Preservation of MeCP2 function in forebrain GABAergic neurons restores auditory processing in *Mecp2*-null mice
(a) Heat maps showing changes in event-related power in response to 85-dB white noise sound presentation as a function of time and frequency. **(b)** Population averages of event-related power for *Mecp2^{Stop/y}; Dlx5/6-Cre* (n = 11), *Mecp2^{Stop/y}; Emx1-Cre* (n = 6) and *Mecp2^{Stop/y}* mice (n = 9). Frequency bands correspond to: δ , 2–4 Hz; θ , 4–8 Hz; α , 8–12 Hz; β , 12–30 Hz; γ_{low} , 30–50 Hz; γ_{high} , 50–90 Hz; ϵ , 90–140 Hz. Shaded regions represent s.e.m. Top blue line represents those regions with FDR < 0.05 (permutation test).

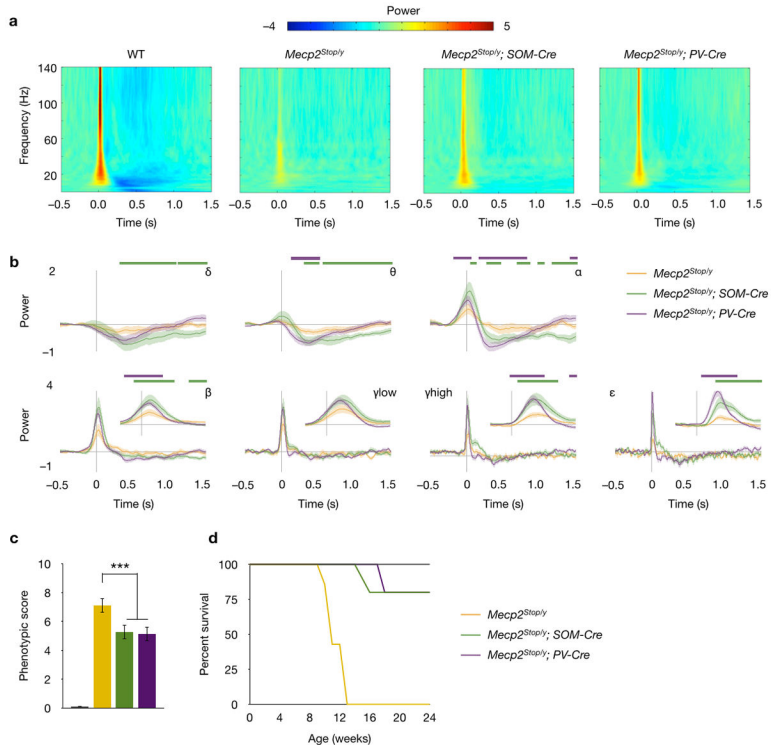


Fig. 3. Preservation of MeCP2 function in either SOM- or PV-expressing interneurons leads to a partial restoration of auditory processing

(a) Heat maps showing changes in event-related power in response to 85-dB white noise sound presentation as a function of time and frequency. (b) Population averages of event-related power for *Mecp2^{Stop/y}; PV-Cre* (n = 7), *Mecp2^{Stop/y}; SOM-Cre* (n = 12) and *Mecp2^{Stop/y}* mice (n = 9). Frequency bands correspond to: δ , 2–4 Hz; θ , 4–8 Hz; α , 8–12 Hz; β , 12–30 Hz; γ_{low} , 30–50 Hz; γ_{high} , 50–90 Hz; ϵ , 90–140 Hz. Shaded regions represent s.e.m. Top green or purple bars represent those regions with FDR < 0.05 (permutation test) in SOM- cre or PV-cre mice, respectively. (c) Phenotypic scoring of mice at 12 weeks of age (n = 8 per genotype). *** corresponds to a p-value < 0.001, one-way ANOVA with *post hoc* Tukey. (d) Survival curves for mice (n = 8 per genotype).